

CERN - PS DIVISION

PS/RF Note 2002-039

# Measurement of the Longitudinal Coupling Impedance for the PS Electrostatic Septum 31

A. Mostacci

## ABSTRACT

In the frame of general PS-machine impedance evaluation the septum PESEH31 has been measured using the classical coaxial wire method. Potentially dangerous resonances were identified and remedies are proposed.

Geneva, Switzerland  
March 2002

## 1 Introduction and motivation

A constant and persistent effort is required to improve whenever possible the beam coupling impedance of all PS machine elements. This is due to the fact that the PS machine has undergone many upgrades during its evolution over the past decades. As a consequence the beam intensity has been augmented by several orders of magnitude and bunch lengths became shorter. Obviously more stringent requirements for the impedance budget result from these improvements. Since there are nearly always certain elements of the PS machine taken out for repair or upgrade, one has to use the opportunity the measure the impedance on the bench and if required, implement or foresee further improvements.

In the framework of the consolidation project of the electrostatic septa in the PS ring [1], the first tank of septum PESEH31 became available for impedance bench measurements during February 2002. Usually the measurement job is not at all straightforward since it requires individual adaptation for the particular Device Under Test (DUT). Anyway, for this particular case, we profited by the experience gained in analogous measurements done on PESEH23 [2], also reusing hardware pieces (e.g. external flanges to support the wire) already developed at that time. The geometries of the two septa are (with respect to electrical aspects) similar except one important difference that will be discussed in details later in sec. 3. On top of that, PESEH31 already implements the improved septum/flanges contacts proposed in [2] for the PESEH23, giving the opportunity to experimentally check their effect.

Usual techniques and advises to correctly perform impedance bench measurements are summarised in [3]. In the present paper we report about the results of measurements of the longitudinal coupling impedance by means of the “coaxial wire method”. A description of the actual set-up, the measurement procedure and its outcomes are given in sec. 2 while sec. 3 highlights the most interesting results and discusses some possible future improvements.

A photo of the septum C-support inside the device is shown in Fig. 1 (left picture); the openings on the right hand side of the C-support are pumping holes. In the following we refer to the septum as the whole device and not strictly the molybdenum foil which is the “active part” and it is situated just after the wires (right picture). The septum is contained in a tank with circular flanges which have to be electrically connected with the septum itself. For this purpose, some RF-fingers are mounted on the septum extremity: they are a crucial item as pointed out in [2] and briefly discussed in sec. 3.

## 2 Measurements

A copper wire is placed on the axis of the DUT and a Vector Network Analyser (VNA) measures the transmission coefficient  $S_{21}$  between the two extremities. The measurements are performed with a copper wire having a diameter of 0.4 mm. The wire is aligned to the theoretical beam (orbiting) axis; in general this is not the centre of the elliptical vacuum chamber, since during machine operation the chamber inside the septum is moved due to machine optics requirements. The measurements have been carried out on PESEH31 in different conditions, i.e. with various horizontal offsets between the flange centre and the ellipse centre.

The coaxial transmission line formed by DUT + wire is mismatched with respect to the instrument (VNA, 50  $\Omega$  generator and load impedance) and some matching resistors have been used. The coupling impedance can be computed from the transmission



Figure 1: Relevant Geometry. The left picture shows the inside part of the septum tank with the nearly elliptical septum C-support and the wires. Pumping holes are visible in the right part of the pipe. The right picture shows an enlarged view inside the tank, close to the septum foil. The wires and the molybdenum foil are separated by a slot.

parameter  $S_{21}$  via the “logarithmic formula”:

$$Z_{log} = -2Z_c \ln \left( \frac{S_{21}^{DUT}}{S_{21}^{REF}} \right) \quad (1)$$

where  $Z_c$  is the characteristic impedance of the coaxial line and  $S_{21}$  is the transmission coefficient (measured by the VNA). REF stands for REFerence measurement; such a reference measurement in a smooth, homogeneous beam pipe has not been done for practical reasons. We assumed, instead, for the reference a lossless line of length  $L$  (that is  $S_{21}^{REF} = e^{-j\omega L/c}$ ) where  $L$  is the mechanical distance between the connectors joining the wire extremities with the cables from the network analysers. This delay has been included in the raw data via the time delay correction function of the network analyser; thus, all the  $S_{21}$  data discussed/used in the following are meant to be  $S_{21}^{DUT}/S_{21}^{REF}$ . After having described the basic steps of the method, we will now report on the actual results.

In order to get the correct value of the matching resistor, we need a measurement of the impedance  $Z_c$  of the wire in the DUT. Then, the resistance  $Z_{match}$  satisfies simply the matching condition [4]:

$$Z_c = Z_{match} + 50 \Omega.$$

To measure  $Z_c$  we performed a kind of “Time Domain Reflectometry”, using the time domain option of the HP8753D network analyser. We measured the signal reflected by the unmatched transmission line with a synthesised (unitary) step excitation, the so called “low frequency step” in the VNA jargon. The calibrated  $S_{11}$  for the (unmatched) coaxial line is shown in Fig. 2 as a function of the delay along the transmission line; the different “stairs” are the multiple reflections at the opposite ends of the structure. Each plateau has the same typical undulation due to periodically spaced lateral venting holes (about 4 cm diameter) in quasi-elliptical beam pipe inside the septum tank. From the amplitude  $\Delta\Gamma$  of the reflection coefficient it is possible to get the impedance of the line  $Z_c$ , i.e.

$$Z_c = Z_0 \frac{1 + \Delta\Gamma}{1 - \Delta\Gamma} = Z_0 \frac{1 + 0.664}{1 - 0.664} = 248 \Omega, \quad (2)$$

since  $Z_0 = 50 \Omega$ . Accordingly,  $Z_{match} = Z_c - Z_0 = 198 \Omega$ ; for practical reasons, then, the two matching resistors actually soldered between the wire and the connectors are of  $200 \Omega$ .

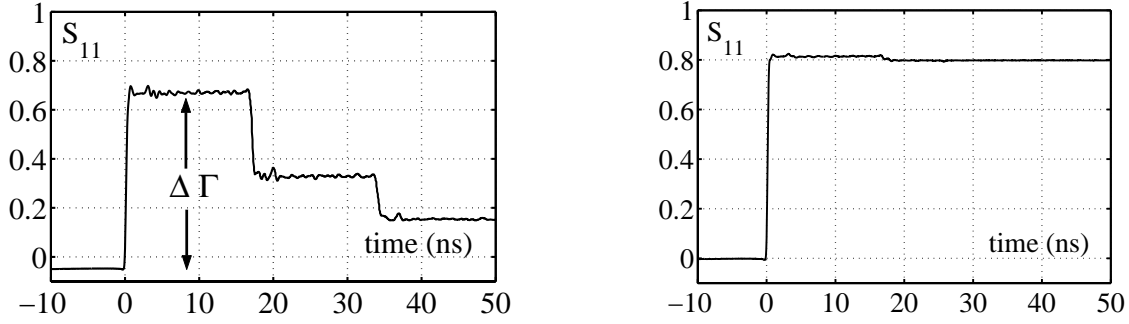


Figure 2: Reflection coefficient measurements in the time domain. The left plot shows multiple reflections in the non-matched coaxial line obtained by inserting a wire (0.4 mm diameter) along the DUT axis. Adding matching resistors (computed from  $\Delta \Gamma = 0.664$ ), the multiple reflections disappear at the expenses of an increased reflection between DUT and instrument (right plot).

After soldering the matching resistors on each side of the copper wire, the transmission coefficient  $S_{21}$  looks like in Fig. 3. The upper plot shows its magnitude (in dB) when the low frequency ohmic losses on the matching resistor are corrected away. The lower plot shows the phase of  $S_{21}$  after the time delay correction according to the (mechanical) length of the line (which is roughly 2.57 m, i.e. longer than PESEH23). To get Fig. 3, the

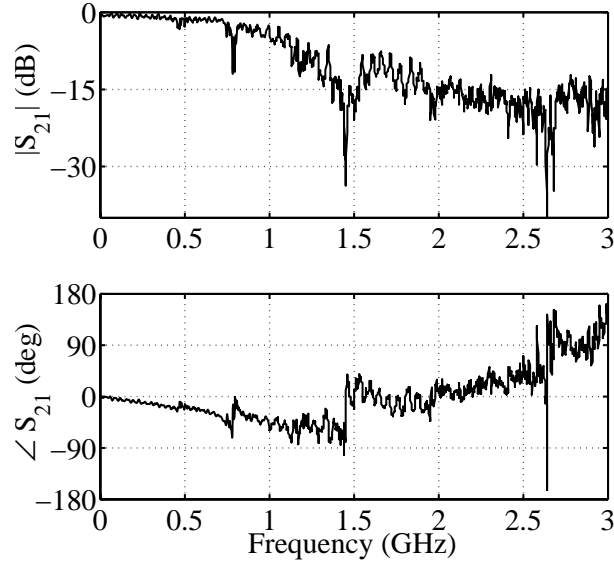


Figure 3: Transmission coefficient ( $S_{21}$ ) versus frequency. A copper wire (0.4 mm diameter) is placed along the DUT axis. Matching resistors have been mounted at each end of the wire. The amplitude (upper plot) has been corrected from the low frequency losses on the resistors. The lower plot shows the phase of the  $S_{21}$  after “time delay connection” (2.57 m).

raw data for  $|S_{21}|$  are shifted up (so that  $|S_{21}| = 0$  at low frequencies) in order to subtract

the ohmic losses on the matching resistors. Unfortunately, such losses changes with frequencies and this explains partially the strong decreasing of the  $|S_{21}|$  at high frequencies (i.e. above 1 GHz). In fact, for it has been used a high precision resistor (1% uncertainty on its nominal value) which has a strong parasite impedance at high frequencies. Massive carbon resistors (5% uncertainty on their nominal value) are better suited for this kind of measurements; unfortunately, when we realised, the septum was not anymore available for measurements. In principle this effect could have been also calibrated away with a reference measurement of the wire (with the resistors) in a perfectly conducting pipe.

A detailed view of the two main notches (780 MHz and 1.45 GHz) is given in Fig. 4. These resonances are due to the coupling with the tank modes via a big hole placed in the septum foil (which was not the case in PESEH23). In fact the continuous thin foil in PESEH23, here is replaced by (going in the beam direction) first some wires, then a “big hole” and eventually the molybdenum foil. Such a hole (azimuthally bigger than the venting holes in the opposite side) was used in the early days to house a pick-up coil, presently dismantled. For the propagation of image currents, this hole represents a big obstacle because of its azimuthal extension and then its contribution to the coupling impedance is relevant. On top of that, such a hole is quite efficient in exciting tank modes and this explains the typical resonant pattern. The other notches at high frequency (around 2.5 GHz and above) are the signature of higher order propagating modes.

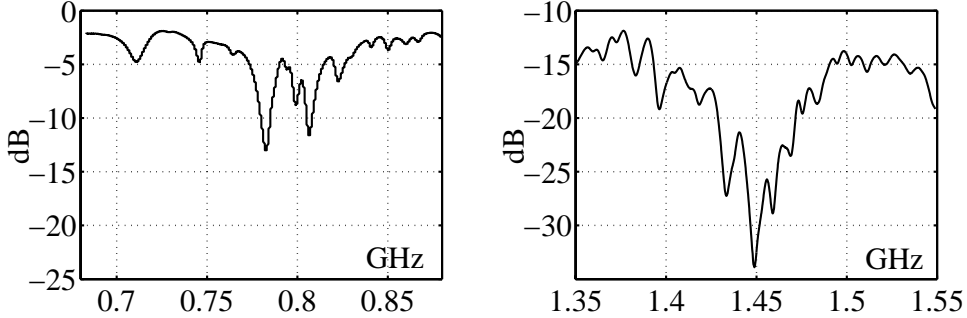


Figure 4: Transmission coefficient ( $|S_{21}|$ ) versus frequency for the two main resonances.

The longitudinal coupling impedance can be calculated using the raw data of the transmission coefficient in Eq. (1) with Eq. (2); its real part  $Z_{real}$  is shown in Fig 5. The peaks (pointed by the arrows) correspond obviously to the notches of the  $|S_{21}|$  discussed above. This is quite a strong effect and having identified them is the most important outcome of the bench measurements which we are reporting about. The coupling impedance at the resonances (roughly a  $k\Omega$ ) and the  $Q$ -factor (about few hundreds) are quite high; the peak frequencies (780 MHz and 1.45 GHz) are such that they may represent a problem for the beam stability in the PS. The strong increase of the impedance (corresponding to the strong decrease in  $|S_{21}|$ ) may be partially due to reactive/inductive effects in the matching resistors.

### 3 Comments

A comparison with the similar septum PESEH23 is straightforward. They differ only in the mechanical length (PESEH23 is only 1.1 m long) and in the septum foil geometry: PESEH23 has a continuous foil, while PESEH31 has a more complicated geometry with wires, foil and the hole discussed above. Following the recommendations given in [2],

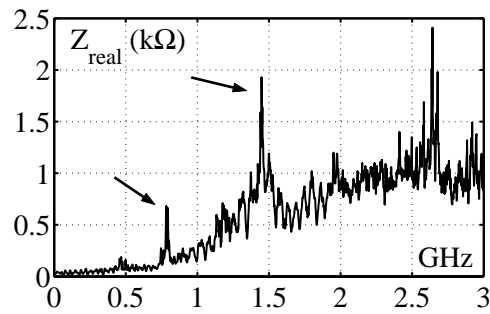


Figure 5: Real part of the longitudinal coupling impedance according to the “log formula”. A copper wire (0.4 mm diameter) with matching resistors has been used. Dangerous resonant modes are pointed by the arrows.

the PS/PO group have already equipped PESEH31 with an improved version of the RF contacts between the septum itself and the flanges (as shown in Fig. 6). As a matter of

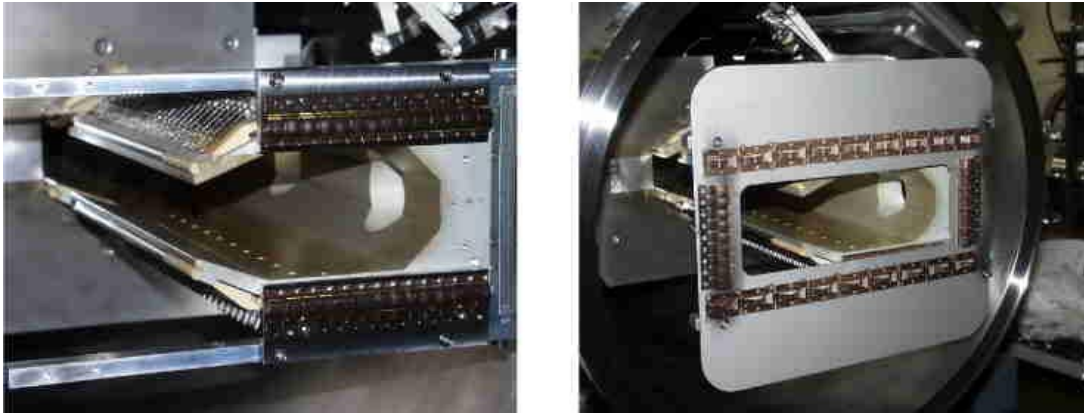


Figure 6: Detailed view of the RF contacts between septum and external flanges.

fact, the coupling impedance peaks measured on the PESEH23 and attributed to parasite cavities in the contact region have not been measured (about  $200 \Omega$  around 590 MHz and about  $400 \Omega$  around 1.39 GHz) in PESEH31. On top of that to prove that the resonances are due to the septum geometry (in particular to such a hole),  $S_{21}$  measurements have been taken in two different positions of the septum (at the extremities of the possible moving range). The ratio (in dB) of the transmission coefficient is shown in Fig. 7; it is remarkably different from 1 (i.e. 0 dB) mostly at the resonance frequencies. Thus the impedance peaks of Fig. 5 are not due to contacts (which are independent from the position of the septum), but to the shape of the septum itself; in particular, we believe, they are due to such a big hole (see Fig. 1) which couples the septum to the external tank. Closing completely the hole seems to be the best choice, but it is also practically very difficult without a major intervention on the whole septum. A much easier solution which may accommodate both impedance budget requirements and feasibility limitations is to partially shield the hole only on the top and on the bottom. It is feasible because the geometry along the beam path between wires and the foil (where the alignment is critical) is not changed, and it will reduce the hole to about the size of the venting holes (which are not harmful). A further improvement may include putting some adsorbing material in the tank (and away from the maximum electrostatic deflecting field regions) to enhance

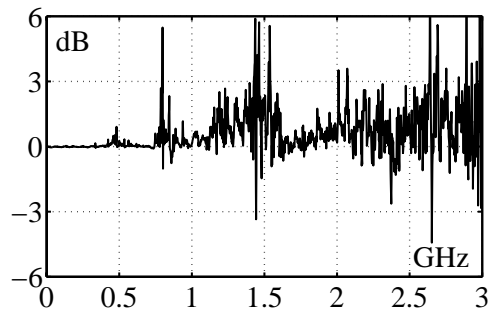


Figure 7: The plot shows the ratio of the  $|S_{21}|$  parameters measured with the septum in two different positions (i.e. after the maximum possible translation). The difference is relevant only in proximity of the resonance frequencies.

losses for the parasite tank modes.

#### 4 Conclusion

The longitudinal beam coupling impedance of the first tank of the septum PESEH31 has been evaluated using the coaxial wire method. As a result two major resonances were found at 780 MHz and 1.45 GHz; they were attributed to a hole used in the early days to house a pick-up coil. Such resonances may be dangerous for PS beam stability and an action to reduce/eliminate them should be foreseen by, for instance, reducing the hole size. The tank of the septum PESEH31 studied has been equipped with an improved version of RF contacts between the septum and the flanges, as suggested in [2] concerning PESEH23. The measurements reported above confirm the beneficial effect of such new contacts since the resonances measured in PESEH23 disappeared.

#### 5 Acknowledgements

This work profited of many suggestions by F. Caspers, who taught me practically everything I know, about coupling impedance bench measurements. I would like to thank J. Borburgh, M. Hourican and A. Prost for all their help during the setup of the bench tests and for the writing of this report. Thanks are also to R. Garoby and A. Blas for support.

#### References

- [1] J. Borburgh, M. Hourican, M. Thivent, *Consolidation project of the electrostatic septa in the CERN PS ring*, IEEE Particle Accelerator Conference, Chicago, IL, USA, 18–22 Jun 2001, to be published; see also CERN-PS-2001-024-PO, June 2001.
- [2] F. Caspers and A. Mostacci, *Measurements of the longitudinal coupling impedance for the PS electrostatic septum 23*, PS/RF Note 2001-012, CERN, September 2001.
- [3] F. Caspers, *Impedance Determination from Bench Measurements*, Handbook of accelerator physics and engineering, A.W. Chao and M. Tigner (editors), World Scientific, Singapore, 1999.
- [4] F. Caspers, A. Mostacci and B. Spataro, *On trapped modes in the LHC recombination chambers: experimental results*, LHC Project Note 266, CERN, August 2001.